Funded by the European Union's
Horizon Europe programme under
the grant agreement No 101096487

D5.1 Control System design for the dynamic model

WP5 Control Avionics

Disclaimer

Document Information

Grant Agreement / Proposal ID	101096487
Project Title	AUTONOMOUS FLYING SHIPS FOR INTER-ISLAND AND INLAND WATERS TRANSPORT
Project Acronym	AIRSHIP
Project Coordinator	Universidad Politécnica de Madrid
Project starting date (duration)	1st January 2023 (48 months)
Related Work Package	WP5 Control Avionics
Related Task(s)	T5.1
Lead Organisation	UPM
Contributing Partner(s)	LU, TAU, TRISOLARIS
Due Date	31/12/2023
Submission Date	30/12/2023
Dissemination Level	PU

Revision History

Revision	Revision Date	Name	Position
1.0	22/12/2023	Sofija Ilic (UPM)	Researcher
2.0	25/12/2023	Matteo el Hariry (LU)	Researcher
2.1	29/12/2023	Pedro Lima (TRISOLARIS)	Researcher
2.2	30/12/2023	Zorana Milosevic (UPM)	Researcher

TABLE OF CONTENTS

List of Tables

List of Figures

Abbreviations and Acronyms

Acronym	Description
AI	Artificial Intelligence
CFD	Computational Fluid Dynamics
CG	Centre of Gravity
CT	Centre of Thrust
DOF	Degree of Freedom
HTP	Horizontal Tailplane
IGE	In Ground Effect
LMI	Linear Matrix Inequality
LQG	Linear Quadratic Gaussian
MPC	Model Predictive Control
NED	North-East-Down
OGE	Out of Ground Effect
PID	Proportional-Integral-Derivative
RBSC	Robust Backstepping Control
RL	Reinforcement Learning
UWV	Unmanned Wing-In-Ground Vehicle
WIG	Wing-In-Ground
WP	Work Package

Table 1: Abbreviation and Acronyms

Funded by the European Union

List of Symbols

Symbol	Description
α	Angle of Attack
β	Side-slip Angle
γ	Heading Angle
V_a	Total Velocity of WIG Vehicle
S	Wing area
b	Wingspan
δ_a	Aileron deflection
δ_r	Rudder deflection
δ_e	Elevator deflection
$\delta_{t1:2}$	Applied Thrust
v^b	Linear velocities in body-fixed frame
ω^b	Angular velocities in body-fixed frame
p^n	Position of centre of mass of the vehicle in NED frame
Θ	Euler angles in NED frame
F_g^b	Vector of forces of gravity
F_{aero}^b	Vector of aerodynamic forces
$F_{t_{1:2}}^b$	Vector of thrust forces
T_{aero}^b	Vector of aerodynamic moments
C_D	Drag Aerodynamic Coefficient
C_L	Lift Aerodynamic Coefficient
C_Q	Side force Aerodynamic Coefficient
C_l	Rolling Moment Coefficient
C_m	Pitching Moment Coefficient

Funded by the European Union

Symbol	Description
C_n	Yawing Moment Coefficient
$J = \begin{bmatrix} J_{xx} & J_{xy} & J_{xz} \\ J_{yx} & J_{yy} & J_{yz} \\ J_{zx} & J_{zy} & J_{zz} \end{bmatrix}$	Inertia Matrix
θ	Pitch Angle
ψ	Yaw Angle
ϕ	Roll Angle

Table 2: List of Symbols

List of System Parameters for AIRSHIP-1

Symbol	Description	Value
ρ	Air Density	$1.225\ kg/m^3$
v_c	Cruise Speed	$28\ m/s$
b_w	Span (Wing)	$5\ m$
b_h	Span (HTP)	$2.74\ m$
AR_w	Aspect Ratio (Wing)	7.5
AR_h	Aspect Ratio (HTP)	$7/6$
TR_w	Taper Ratio (Wing)	$0/4$
TR_h	Taper Ratio (HTP)	0.85
S_w	Wing Area	$3.384\ m^2$
S_h	Horizontal Tail plane Area	$0,994\ m^2$
h_{CG}	CG Altitude from Surface	$0,495...10\ m$
e	Napier's Constant	2.71828
e_{0w}	Oswald's Efficiency Factor (Wing)	0.9

Funded by the European Union

Symbol	Description	Value
e_{0h}	Oswald's Efficiency Factor (HTP)	0.9
π	Pi	3.14159
C_{D0}	Zero Lift Drag Coefficient	0.0306
α	Angle of Attack	$-5°...8°$
α_{0w}	Zero Lift Angle of Attack (Wing)	$-3,5°$
α_{0h}	Zero Lift Angle of Attack (HTP)	$-4,5°$
i_w	Angle of Incidence (Wing)	$4,75°$
i_h	Angle of Incidence (HTP)	$2,5°$
ϵ	Down wash Angle (HTP)	$0°$
m_t	Maximum take-off weight	$112\ kg$
m_t	Mean Aerodynamic Chord Length	$0,646\ m$
h_{ss}	Steady-State Height	$0,93\ m$
θ_{ss}	Steady-State Pitch Angle	$0°$
J_{A1}	Inertia Matrix	$\begin{bmatrix} 39,71 & 0 & 8,97 \\ 0 & 85,51 & 0 \\ 8,97 & 0 & 114,39 \end{bmatrix}$
$Stall_{AOA}$	Stall Angle Of Attack	$13°$
C_Q	Side Forces Coefficient	$0,019$
C_m	Pitching Moment Coefficient	$-0,02$
C_n	Yawing Moment Coefficient	$-0,002$
$[\delta_a^{min}, \delta_a^{max}]$	Aileron Deflection limits	$[-20,15]°$
$[\delta_e^{min}, \delta_e^{max}]$	Elevator Deflection limits	$[-20,20]°$

Funded by the European Union

Symbol	Description	Value
$[\delta_r^{min}, \delta_r^{max}]$	Rudder Deflection limits	$[-15, 15]^\circ$
δ_t^{max}	Maximum Thrust Force	$219\ N$
CG	x position of CG	$0\ m$
CG	y position of CG	$0\ m$
CG	z position of CG	$0\ m$
CT	x position of CT	$-0,052\ m$
CT	y position of CT	$-0,58/0,58\ m$
CT	z position of CT	$0,28\ m$

Table 3: List of System Parameters for AIRSHIP-1

Executive Summary

This deliverable contains the findings of the research activities devoted to system modelling, simulations and control strategies in order to achieve autonomous Guidance, Navigation and Control of the WIG vehicle. Starting from the description of the dynamical model of the airship vehicle, this deliverable will describe control strategies in order to achieve an automatic operation.

The outcome of this deliverable will provide inputs for upcoming tasks: T5.2 (WIG 6 DOF Control) and T5.3 (WIG Software-in-the-loop and Hardware-in-the-loop Simulations).

Funded by the European Union

1 Introduction

There are many archipelagos and intercontinental waterways in Europe which are used daily to transport goods and people. The use of airplanes and ships for these purposes requires enormous amount of energy, financial and human resources. Therefore, designing a new mode of transportation to comply with upcoming EU regulations on net-carbon reductions for maritime transport, and reducing the consumption of non-renewable resources served as a primary inspiration for this work. To respect these new regulations, and match the ever-growing demand for fast and reliable shipping, new innovative solutions are required. AIRSHIP iterates on the little-known Wing In Ground effect vehicles. This concept, dating from the mid-50s USSR, allows fast and efficient transport of goods. In the middle of the twentieth century, Rostislav Alekseyev designed and created a powerful vehicle called Caspian Sea Monster (Komissarov & Gordon, 2020) that was solely designed for military purposes. With this concept, he laid the foundation for ekranoplans also known as Wing-In-Ground vehicles. These vehicles use the ground effect to increase the lift force while reducing the drag force. The result is a vehicle capable of flying at high speeds with increased energy efficiency while being able to transport heavy loads. However, due to marginal stability, Wing-In-Ground vehicles are particularly challenging for humans to maneuver. This means that even a small piloting error can lead to terrible incidents. This is one of the core motivations behind the development of a fully autonomous WIG vehicle. Additionally, autonomous vehicle control offers several benefits that contribute to improved safety, efficiency, and convenience, such as optimized traffic flow, increased fuel and time efficiency and mobility and accessibility of resources. Designing a control system that ensures the autonomy of the Wing-In-Ground vehicle would open numerous opportunities for such vehicles. Enabling their use in a wide range of applications and services, and eliminating the human error factor, thus realizing greater safety and at the same time ensuring superior energy efficiency.

1.1 Purpose of the deliverable

The deliverable D5.1 focuses on the conceptualization and design of the control system for Wing-In-Ground (WIG) vehicles. Its primary objective is to present a mathematical model of flight dynamics for the WIG vehicle, along with proposing potential control strategies. It includes an overview of related work, methodology, the mathematical model developed for this purpose, an introduction to potentially suitable control strategies, followed by conclusions and prospects for future work.

D5.1 describes the outcomes of Task T5.1 (WIG System Modelling), setting the foundation for subsequent tasks, T5.2 (WIG 6 DOF Control) and T5.3 (WIG Software-in-the-loop and Hardware-in-the-loop Simulations). In task T5.2, the main goal is to investigate the possibilities of implementing control strategies based on the knowledge and experience gained, as well as keeping in mind the system's capabilities and constraints. In task T5.3 the designed control system will be tested in various software- and hardware- in the loop scenarios.

This deliverable is intrinsically linked with WP3, as the selected design and parameters of the WIG vehicle directly influence its modeling. The model will be refined in tandem with the vehicle's design enhancements. Specifically, post the wind tunnel and water channel testing, the gathered data will be utilized to refine the aerodynamic and hydrodynamic coefficients. At this project stage, the primary focus is on in-ground-effect flight, with hydrodynamic simulations scheduled for later phases.

Besides WP3, D5.1 is linked to other technical WPs of the project. It outlines control strategies that integrate perception for obstacle-free navigation (WP6) and contributes to the overall Guidance, Navigation, and Control (GNC) system (WP7). The control algorithms must be designed to efficiently manage power demands for specific manoeuvres, addressing power surges and consumption (WP4). Ultimately, the control algorithms and strategies developed in D5.1 will be integrated into the AIRSHIP-1 vehicle, undergoing validation in flight tests (WP8), thereby demonstrating their practicality and effectiveness in real-world scenarios.

1.2 Document Structure

In order to design a controller for a complex dynamical system, we first need to model it properly. Hence, in this document, we start by presenting the dynamics of WIG vehicles and their physical properties. Then, we provide details on such model of the dynamical system and briefly introduce its integration in the two simulation environments we are building: a MATLAB simulator for traditional control techniques and system stability analysis, and a Python one, for AI based control strategies. Finally, with the equations of dynamics known, we propose possible strategies that can be adapted for WIG vehicle flight control.

2 WIG Vehicle Dynamics

To better understand the principles of WIG Vehicle flight, this section presents the underlying system dynamics that governs the movement of this vehicle in the atmosphere. First, it is important to analyse the forces acting on the WIG Vehicle while flying. There are four forces that act on any object in flight, namely: lift force, drag force, thrust force and gravity force. The forces of lift and gravity act in the vertical plane of the object, while the force of drag and the thrust act in the horizontal plane of the object, as shown in the figure 1.

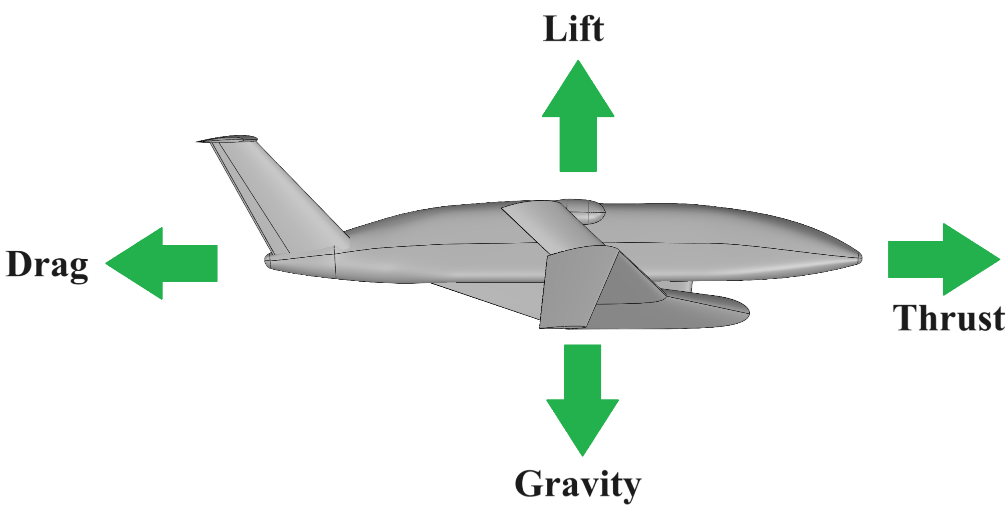

Figure 1: Illustration of forces acting on an WIG Vehicle in flight

Force of lift is the main aerodynamic force that tends to keep an object in the air, opposing the force of gravity that tends to bring the object down to Earth. The force of lift is the pressure that needs to be applied to overcome the force of gravity. How much pressure should be applied depends on the weight of the object itself. Also, the faster the aircraft moves, the greater the thrust force. On the other hand, in the horizontal plane of the object, we have the forces of drag and the thrust force. Drag is a mechanical force that occurs when a solid object interacts with a fluid, while the thrust force is generated by the engine that serves to propel the aircraft forward.

In addition to the described forces, it is also important to define the effect of the ground effect, which is crucial for the dynamics of the WIG Vehicle. The ground effect is a phenomenon of increasing lift and decreasing drag when the aircraft is close to the ground. This phenomenon is due to the distortion of the air flow under the wing and can be attributed to the proximity of the ground. An illustration of the operation of the ground effect is shown in Figure 2.

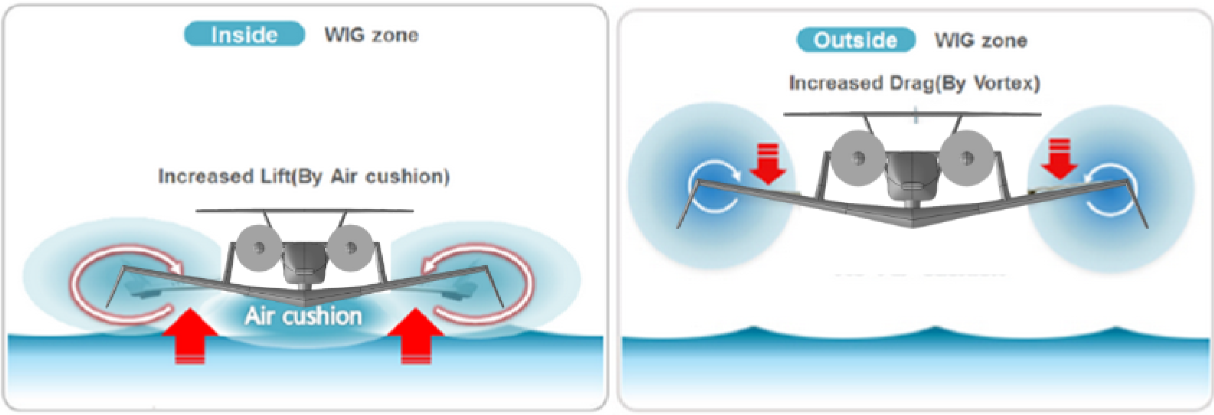

Figure 2: Illustration of the ground effect

In general, WIG vehicle can move along three axes of translation, as well as rotate around three axes. Rotation is described by Euler angles, better known as pitch, roll and yaw, shown in Figure 3.

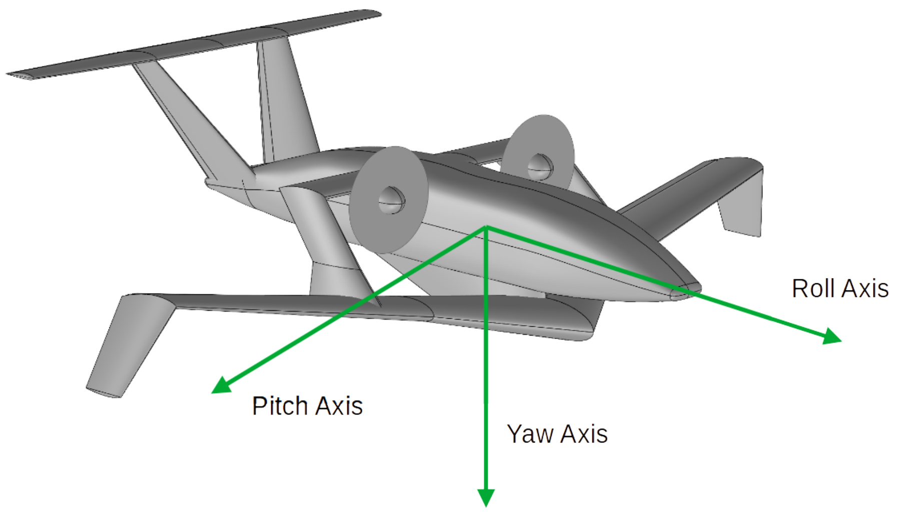

Figure 3: Illustration of the possible rotations around three axes

2.1 Vehicle Stability

Stability analysis is an essential aspect of control systems engineering. It involves the evaluation of a system's behavior over time and its response to external disturbances. Stability analysis is crucial in ensuring that a control system operates optimally. It helps identify whether the system will remain stable under various external forces. The purpose of controller stability analysis is to determine the range of controller gains between lower and upper limits that lead to a stable controller.

The stability of the WIG vehicle can be analysed and described with two types of stability - static and dynamic stability (Yun, Bliault, & Doo, 2010b). Static stability refers to the initial tendency of the object's behaviour during disturbance and can be positive, negative or neutral, while dynamic stability refers to the tendency of the object's behaviour over time. To ensure dynamic stability, it is necessary to primarily ensure positive static stability. Positive static stability can be divided into three types of stability considering the three axes of rotation - longitudinal, lateral and directional stability. Longitudinal stability represents the ability to stabilize the aircraft after disturbances in the pitch angle, lateral stability represents the ability to stabilize the aircraft after disturbances in the roll angle, while directional stability represents the ability to stabilize the aircraft after disturbances in the yaw angle.

Analyzing the stability of a control system for Wing-in-Ground vehicles involves assessing the dynamic behavior of the system to ensure that it remains stable under various operating conditions. The fundamental approach for evaluating the stability of an automatic control system involves solving its linear differential equation of motion. However, computing the roots of the characteristic equation is not always convenient. Consequently, automatic control theory has devised specialized methods known as stability criteria. Algebraic criteria enable the assessment of the stability of an automatic control system by analyzing its parameters, which are determined by the coefficients of its characteristic equation. In contrast, frequency criteria offer specific advantages over algebraic criteria. Firstly, there is no need to solve systems of differential equations, particularly those of higher orders. Secondly, these criteria provide clarity. Thirdly, they allow for the utilization of experimentally determined frequency characteristics of systems. By employing frequency criteria, one can make decisions about measures to ensure the stability of the system without the necessity of solving complex differential equations, particularly when indications suggest instability.

Establishing a mathematical model that describes the dynamics of the WIG vehicle in this deliverable sets the foundation for stability analysis of the control system which can be performed in following way:

- Linearizing the nonlinear equations of motion around the desired operating point to create a linear model which simplifies the analysis and allows for the application of linear control system techniques.
- Obtaining the transfer function representation of the system which involves transforming the linearized equations into the Laplace domain, allowing frequency-domain analysis.
- Applying stability criteria, such as the Routh-Hurwitz criterion or Nyquist criterion, to analyze the stability of the system. These criteria provide insights into the system's stability based on the locations of poles in the transfer function.
- Using frequency domain analysis techniques, like Bode plots, to analyze the system's response to different frequencies. This helps in understanding how the control system behaves across a range of frequencies.
- Performing root locus analysis to visualize how the system's poles move as a controller parameter is varied. This is particularly useful for understanding the impact of control gains on stability.
- Analyzing the eigenvalues of the state matrix to assess stability. Eigenvalues should have negative real parts for stability.
- Simulating the system response to step, impulse, or other input signals in the time domain. Evaluating the transient and steady-state response to ensure stability.
- Assessing the robustness of the control system by considering variations in parameters, external disturbances, and uncertainties. Evaluating how well the system can maintain stability in the presence of these factors.
- Validating the stability analysis through simulation and, if feasible, through physical testing of the WIG vehicle with the implemented control system. Simulation can help identify potential issues before physical testing.
- Ensuring that the control system design and performance comply with relevant standards and regulations for WIG vehicles.

In the existing literature one can find various stability analysis techniques such as (Collu, Patel, & Trarieux, 2007) in which several dynamics model for aircraft and WIG crafts are described to determine their stability in different situations such as aerodynamic mode, hydrodynamic mode and hybrid mode or (Aminzadeh & Khayatian, 2017) where stability is analysed for time-varying WIG craft dynamics in the presence of wavy boundary and gust. (Fevralskikh & Makhnev, 2023) describes how rotary derivatives of aerodynamic characteristics, which are are determined using numerical simulations based on the Reynolds-averaged Navier-Stokes equations, are used to study the dynamics and stability of WIG vehicles. Speaking of longitudinal stability requirements for WIG vehicles they have been studied in detail in (Yang, Yang, & Collu, 2015) and (Yun, Bliault, & Doo, 2010a). The stability analysis of WIG vehicles also takes into account the hydrostatic and hydrodynamic forces acting on the vehicle (Park, Hyunbum, 2017). In summary, the following factors should be considered for the stability analysis of WIG vehicles:

- Aerodynamic characteristics
- Longitudinal and lateral motion
- Hydrostatic and hydrodynamic forces
- Control System Stability

It's important to note that stability analysis for WIG vehicles requires a multidisciplinary approach, considering both hydrodynamic and aerodynamic factors. Collaboration between naval, aerodynamic engineers and control systems engineers is essential to comprehensively analyze and enhance the stability of WIG vehicles.

3 Mathematical Modelling

The term mathematical model is fundamental in science and engineering, as it is a very useful and compact way to capture known knowledge about a process. In general, it is not possible to form an entire model based only on knowledge of physical laws, but some parameters are determined by experimental methods. The biggest challenge in mathematical system modelling is the determining the state variables, which essentially describe the dynamics of flow and storage of energy and mass in the system, so positions and velocities are most often used as states. Proposed system modelling principle draw inspiration from various models that can be found in the literature. One of them is Research Civil Aircraft Model (RCAM) (Moormann, Varga, Looye, & Griibel, 1998) which is a twin-engine civil aircraft model developed by the Group for Aeronautical Research and Technology in Europe (GARTEUR). For the purpose of mathematical modelling, this craft is viewed as a rigid body with six degrees of freedom, with possible translation and rotation around the x-, y- and z-axis, which is transferable to mathematical modelling of WIG vehicles. In this chapter, the necessary concepts for understanding and forming the mathematical model of the WIG vehicle will be presented and described in detail, the WIG's equations of motion will be derived and analyzed, and the necessary notation and nomenclature will be established. More precisely, in following sections reference systems, state vector and control surfaces, forces and moments acting on the WIG Vehicle will be defined and a mathematical model in the state-space will be presented.

3.1 Reference Systems

In order to describe the movement of the WIG Vehicle and the forces and moments that act on it, it is necessary to first adopt reference systems in which we will conduct the analysis of dynamics and define the equations of motion of the model itself. In the literature there is a clear agreement regarding which are the reference systems to express the dynamic equations of an 6DOF system. In the same way, the direction of the base vectors of said reference systems are also standardized. The following reference systems used are:

- North-East-Down (NED) Reference System - This is a reference system fixed to the earth and therefore inertial, whose axes are located as shown in Figure 1 below, that is, the x^1-axis pointing north, the y^1- axis pointing east, and the z^1-axis pointing toward the centre of the Earth.

Funded by the European Union

- Reference System fixed to the body - This is a system whose origin is fixed to the centre of gravity of the vehicle. Reference system axes are located as shown in Figure 1 below, x^b pointing in the direction of the nose of the vehicle, y^b pointing to the right wing and z^b pointing downwards.
- Wind Reference System - In this reference system aerodynamic forces can be described in the form of dimensionless coefficients. The x^w-axis is aligned with the velocity vector that is obtained after rotating the y^b-axis according to the angle of attack and the x^b-axis according to side-slip angle explained later.

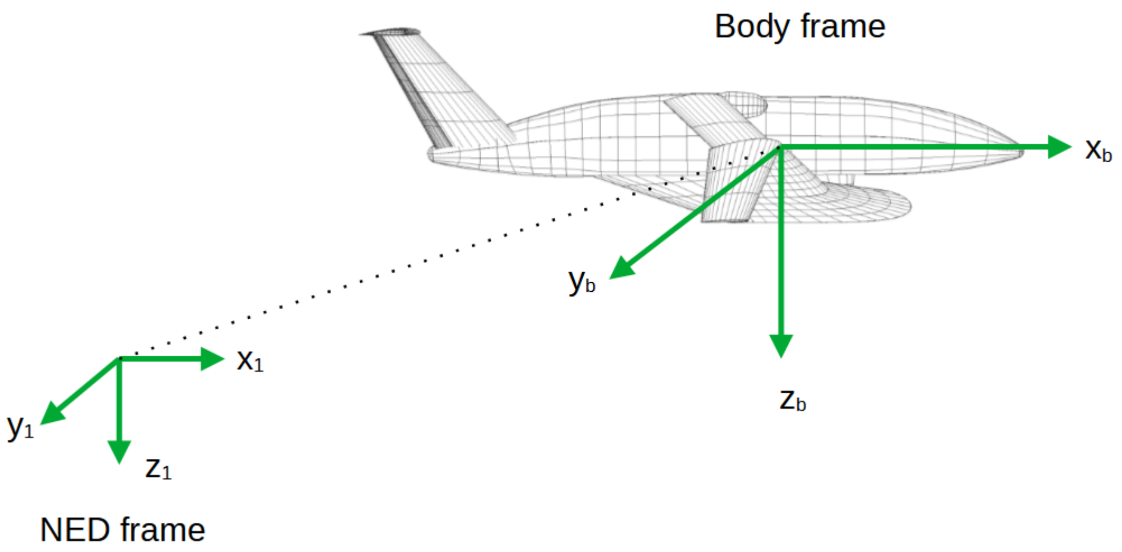

Figure 4: North-East-Down and Body fixed Reference Frames

3.2 Inputs and Outputs of the Control System

3.2.1 State Vector

The variables that characterize the state of the WIG vehicle are:

- Position of the centre of mass of the vehicle expressed in the inertial reference system (NED) - $p^n = [x_c, y_c, z_c]^T$
- Euler angles describe the rotations of the reference system fixed to the body with respect to the inertial reference system (NED) - $\Theta = [\phi, \theta, \psi]^T$
- Linear velocities expressed in the reference system fixed to the body – $v^b = [u, v, w]^T$.
- Air speed V_a, necessary to obtain later calculations, is defined as - $V_a = \sqrt{u^2 + v^2 + w^2}$.
- Angular velocities expressed in the reference system fixed to the body - $w^b = [p, q, r]^T$

Finally, the proposed state vector is

$$x = [u, v, w, \phi, \theta, \psi, p, q, r, x_c, y_c, z_c]^T \tag{1}$$

Here it should be noted that the proposed variables that characterize the state of the vehicle are flexible

Funded by the European Union

and if needed can be adapted into more relevant variables using transformations, i.e. using Quaternions instead of Euler angles, using height of wing or tail instead of absolute altitude etc.

3.2.2 Control Surfaces and Vector

The designed system model has three control surfaces and two engines, as shown in Figure 5. The variables through which the control surfaces and the force exerted by the motor are introduced as:

- Elevator Deflection δ_e - The elevator control surface is positioned horizontally on the tail of the aircraft, as shown in Figure 5. This control surface affects the forces of lift, drag and pitch moment. The actuation range is $[\delta_e^{min}, \delta_e^{max}]$.
- Aileron Deflection δ_a - The ailerons of the vehicle are placed in the wingtips and in a more vertical position than in conventional aircraft. This design aims to facilitate the turning of the vehicle by minimizing the need to roll, which would place it closer to the surface. The actuation range is $[\delta_a^{min}, \delta_a^{max}]$.
- Rudder Deflection δ_r - The rudder is in the rear area of the vehicle, under the elevator. In this design rudders are slightly inclined towards the outside of the vehicle, but the role they play is very close to the ones in conventional aircraft - being the main responsible for controlling the yaw. The actuation range is $[\delta_r^{min}, \delta_r^{max}]$ degrees.
- Thrust Forces δ_{t1} and δ_{t2} - These are the forces exerted by the WIG vehicle engines. For simplification purposes, it will be considered that these forces does not exert any pitching moment and it is carried out purely along x-axis of the vehicle and it pushes it to move. Engine power is controlled as $0 - 1$ percentage of the total achievable force δ_t^{max}.

Control signals' limits $\delta_e^{min}, \delta_e^{max}, \delta_a^{min}, \delta_a^{max}, \delta_r^{min}, \delta_r^{max}$ and δ_t^{max} for this specific design of AIRSHIP-1 prototype are provided in table 3. Finally, the proposed control vector is given as

$$u = [\delta_e, \delta_a, \delta_r, \delta_{t1}, \delta_{t2}] \tag{2}$$

3.3 Aerodynamic Parameters

The key step of modeling WIG Vehicle Dynamics is analysing the aerodynamic effects on WIG vehicle and finding the proper aerodynamic parameters that describe them accurately. In this chapter, aerodynamic angles and coefficients are introduced.

3.3.1 Aerodynamic Angles

Aerodynamic angles are often used for analysis and calculation of aerodynamic coefficients and aircraft motion. Aerodynamic forces should be expressed in the wind reference system since when this reference system is aligned with the direction of the wind, said forces can be treated as dimensionless and expressed in the form of aerodynamic coefficients. The expression of aerodynamic forces and moments in the form of coefficients is very relevant in design. The aerodynamic angles would be:

- Angle of Attack α - It is the angle formed by the direction of the longitudinal axis of the body with the x component of the velocity vector of the body u. It is defined as

$$\alpha = \arctan\left(\frac{w}{u}\right) \tag{3}$$

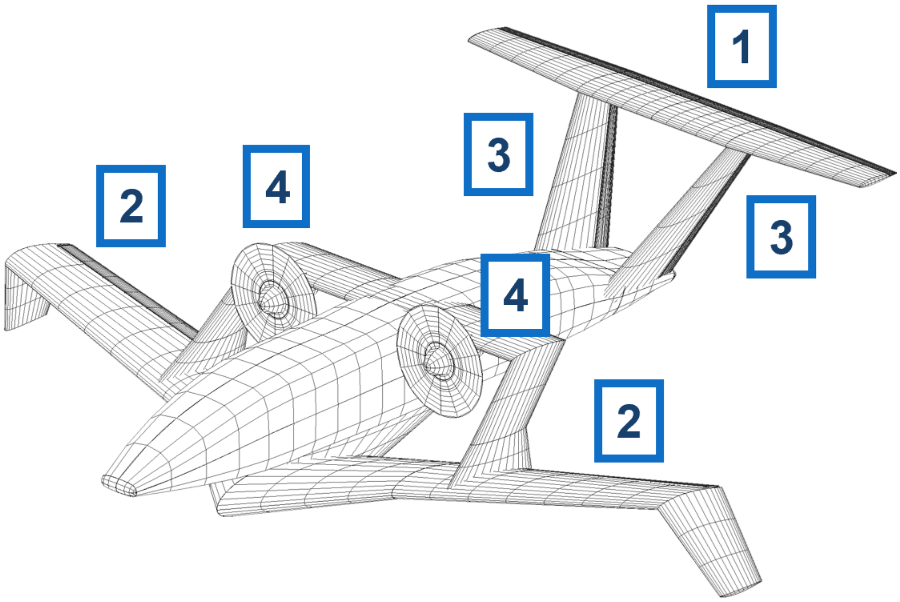

Figure 5: Control surfaces: 1 - elevator, 2 – ailerons, 3- rudders, 4 - engines

- Side-slip Angle β - It is the angle formed by the direction of the longitudinal axis of the body with the y component of the velocity vector of the body v. It is defined as

$$\beta = \arcsin\left(\frac{v}{V_a}\right) \tag{4}$$

- Heading Angle γ - This is the angle formed by the velocity of the center of mass of the aircraft. If it is negative, it would mean that the plane is descending and vice versa. It plays a fundamental role in defining level flight conditions. It is defined as

$$\gamma = \theta - \alpha \tag{5}$$

3.3.2 Aerodynamic Coefficients

The aerodynamic coefficients required for the complete definition of the forces and moments acting on the WIG vehicle will be defined in the following section. Coefficients depend on the achieved height, values of the corresponding angles and control signals. Also, aerodynamic coefficients are significant since they enable the comparison of aerodynamic objects of different sizes, orientations and shapes with the normalization of results considering different forces resulting from different dimensions of objects and flow conditions. Proposed aerodynamic coefficients are based on (Phillips & Hunsaker, n.d.). The dimensionless normalized aerodynamic coefficients describing the aerodynamic forces acting on the WIG vehicle are defined by the following equations.

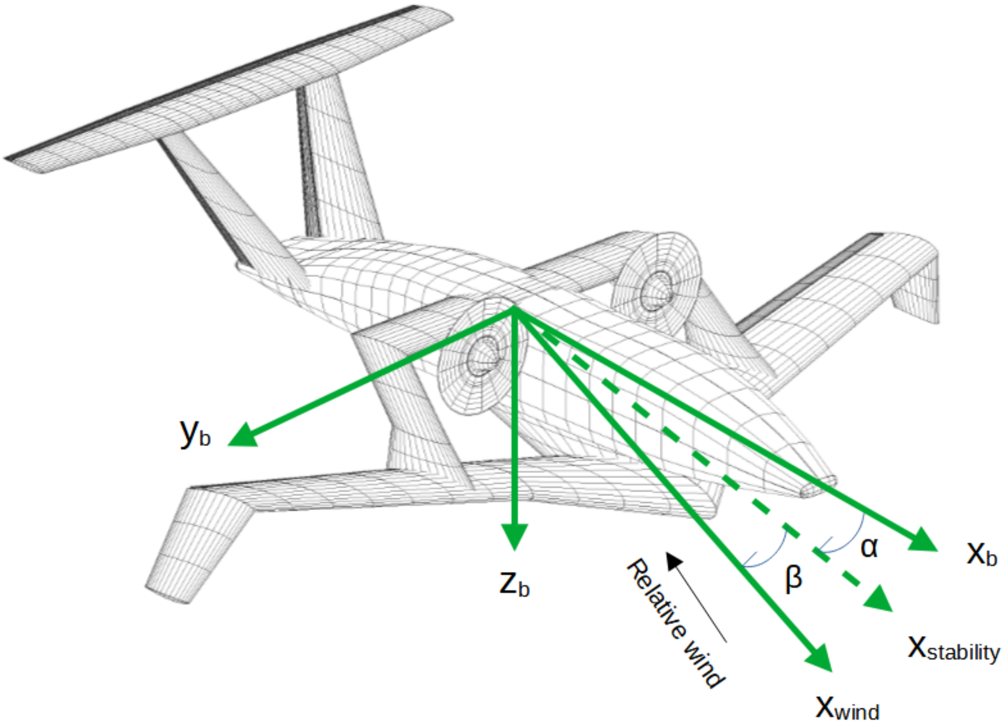

Figure 6: Illustration of Aerodynamic Angles and Reference Frames (Rigon Silva et al., 2017)

Lift Equations:

$$
\begin{gathered}
L_{tot} = L_w + L_h \\
L_w = \frac{1}{2}\rho v_c^2 C_{L_{w,IGE}} S_w \\
L_h = \frac{1}{2}\rho v_c^2 C_{L_{h,IGE}} S_h \\
C_{L_w IGE} = C_{L_{w,OGE}} \mu_{L_w} \\
C_{L_{h,IGE}} = C_{L_{h,OGE}} \mu_{L_h} \\
C_{L_{w,OGE}} = 2\pi \left(\frac{AR_w}{AR_w + 2} \right) (\alpha - \alpha_{0_w} + i_w) \\
C_{L_{h},OGE} = 2\pi \left(\frac{AR_h}{AR_h + 2} \right) (\alpha - \alpha_{0_h} + i_h + \epsilon) \\
\mu_{L_w} = 1 + \left(1 - 2,25\left(TR_w^{0.00273} - 0,997\right)\left(AR_w^{0.717} + 13,6\right)\right) \frac{288\left(\frac{h}{b}\right)_w^{0.787} e^{-9,14\left(\frac{h}{b}\right)_w^{0.327}}}{AR_w^{0.882}} \\
\mu_{L_h} = 1 + \left(1 - 2,25\left(TR_h^{0.00273} - 0,997\right)\left(AR_h^{0.717} + 13,6\right)\right) \frac{288(\frac{h}{b})_h^{0.787} e^{-9.14(\frac{h}{b})_h^{0.327}}}{AR_h^{0.882}} \\
\left(\frac{h}{b}\right)_w = \frac{h_w}{b_w} \\
\left(\frac{h}{b}\right)_h = \frac{h_h}{b_h}
\end{gathered} \tag{6}
$$

where angles $\alpha, \alpha_{0_w}, \alpha_{0_h}, i_h$ and i_w are expressed in radians.

Drag Equations:

$$\begin{aligned} D_{tot} &= D_0 + D_{i_w} + D_{i_h} \\ D_{tot} &= \frac{1}{2}\rho v_c^2 \left(C_{D_0} S_w + C_{D_{i,w,IGE}} S_w + C_{D_{i,h,IGE}} S_h\right) \\ C_{D_{i,w,IGE}} &= \frac{C^2_{L_{w,IGE}}}{\pi e_{0_w} AR_w} \mu_{D_w} \\ C_{D_{i,h,IGE}} &= \frac{C^2_{L_h,IGE}}{\pi e_{0_h} AR_h} \mu_{D_h} \\ \mu_{D_w} &= 1 - (1 - 0.157(TR_w^{0.757} - 0.373)(AR_w^{0.417} - 1.27))e^{-4.74(\frac{h}{b})_w^{0.814}} - (\frac{h}{b})_w^2 e^{(-3.88(\frac{h}{b})_w^{0.758})} \\ \mu_{D_h} &= 1 - (1 - 0.157(TR_h^{0.757} - 0.373)(AR_h^{0.417} - 1.27))e^{-4.74(\frac{h}{b})_h^{0.814}} - (\frac{h}{b})_h^2 e^{(-3.88(\frac{h}{b})_h^{0.758})} \end{aligned} \tag{7}$$

where equations for $C_{Lw,IGE}, C_{Lh,IGE}, (\frac{h}{b})_w$ and $(\frac{h}{b})_h$ are same as in Lift Equations (6). The dimensionless normalized aerodynamic coefficients describing the aerodynamic moments acting on the WIG vehicle C_l, C_m, C_n will be approximated and calculated later on, since the conceptual phase of the project focuses primarily on flying in ground effect and optional hydrodynamic simulations of hydrofoils or hydro skis which will be performed in the later phase of project. For simulation purposes, initial calculations and approximations of system parameters were performed for AIRSHIP-1 in steady state flight.

3.4 Definition of Forces and Moments acting on WIG Vehicle

3.4.1 Forces acting on WIG Vehicle

The total force acting upon the vehicle can be represented as $F^b = F_g^b + F_{aero}^b + F_{t1}^b + F_{t2}^b$, where forces vectors are following:

- **The force of gravity** F_g^b - The vector of forces of gravity in the NED reference system has a single positive component along z -axis, when rotated to the reference system fixed to the body, following force vector is obtained:

$$F_g^b = mg \begin{bmatrix} -\sin\theta \\ \cos\theta\sin\phi \\ \cos\theta\cos\phi \end{bmatrix} \tag{8}$$

- **The aerodynamic forces** F_{aero}^b - The vector of aerodynamic forces is expressed in the wind reference system as the product of air pressure and dimensionless aerodynamic coefficients and adequate rotation matrix:

$$F_{aero}^b = \frac{1}{2}\rho S V_a^2 R_w^b \begin{bmatrix} -C_D \\ C_Q \\ -C_L \end{bmatrix} \tag{9}$$

  where $\frac{1}{2}\rho S V_a^2$ represents aerodynamic pressure and R_w^b the rotation matrix, given by:

$$R_w^b = \begin{bmatrix} \cos\alpha\cos\beta & \sin\beta & \sin\alpha\cos\beta \\ -\cos\alpha\sin\beta & \cos\beta & -\sin\alpha\sin\beta \\ -\sin\alpha & 0 & \cos\alpha \end{bmatrix} \tag{10}$$

- **The thrust forces F^b_{t1} and F^b_{t2}** - For simplification purposes it is considered that the thrust positive forces are acting along the x-axis of the body's reference frame and they are expressed as a percentage of the total force the motor can generate. Following thrust force vectors are obtained, where δ_{t1} and δ_{t2} are the control signals modeled as $0-1$ percentage of the total achievable force $219\ N$:

$$F^b_{t_1} = mg \begin{bmatrix} const \cdot \delta_{t_1} \\ 0 \\ 0 \end{bmatrix} \tag{11}$$

$$F^b_{t_2} = mg \begin{bmatrix} const \cdot \delta_{t_2} \\ 0 \\ 0 \end{bmatrix} \tag{12}$$

3.4.2 Moments acting on WIG Vehicle

For expressing the moments acting upon the vehicle, a simplified model is proposed based on the assumptions that the engines do not exert any type of moment, so the only component that forms the moment vector is the aerodynamic component $T^b = T^b_{aero}$. Moments are expressed in the reference system fixed to the body and can be represented as

$$T^b = T^b_{aero} = \frac{1}{2}\rho S V_a^2 \begin{bmatrix} C_l \\ C_m \\ C_n \end{bmatrix} \tag{13}$$

where ρ is air density, V_a air speed and C_l, C_m and C_n aerodynamic coefficients describing the aerodynamic moments acting on the WIG vehicle.

Final equations that describe forces and moments acting on WIG vehicle can be represented in vector form as:

$$\begin{aligned} F^b &= \begin{bmatrix} X \\ Y \\ Z \end{bmatrix} = \begin{bmatrix} m(\dot{u} + qw - rv) \\ m(\dot{v} + ru - pw) \\ m(\dot{w} + pv - qu) \end{bmatrix} \\ T^b &= \begin{bmatrix} L \\ M \\ N \end{bmatrix} = \begin{bmatrix} J_{xx}\dot{p} - J_{xz}\dot{r} + qr(J_{zz} - J_{yy}) - pqJ_{xz} \\ J_{yy}\dot{q} + pr(J_{xx} - J_{zz}) + (p^2 - r^2)J_{xz} \\ J_{zz}\dot{r} - J_{xz}\dot{p} + pq(J_{yy} - J_{xx}) + qrJ_{xz} \end{bmatrix} \end{aligned} \tag{14}$$

where $J = \begin{bmatrix} J_{xx} & J_{xy} & J_{xz} \\ J_{yx} & J_{yy} & J_{yz} \\ J_{zx} & J_{zy} & J_{zz} \end{bmatrix}$ is the inertia matrix of the WIG vehicle.

3.5 Final System of Equations

The motion of the WIG Vehicle can be described by twelve standard nonlinear differential equations of motion, with possible translation and rotation about the x-, y-, and z-axes, known as the six-degree-of-freedom model (Caughey, 2011) in the following form:

$$\begin{aligned} m(\dot{v^b} + \omega \times v^b) &= F_m \\ J\dot{\omega} + \omega \times J\omega &= M_m \\ \dot{x_i} &= T_{ob} v^b \\ \dot{\Phi} &= R\omega \end{aligned} \tag{15}$$

Funded by the European Union

where the vector Φ represents the Euler angles, v^b represents the velocity vector relative to the object's coordinate system, $\dot{x}_i$ represents the velocity vector relative to the stationary coordinate system (NED), R is the rotation matrix, T_{ob} is the translation matrix and F_m and M_m represent the force vectors acting on the WIG vehicle. In order to derive the mathematical model of the WIG Vehicle in the presented form, it is necessary to adopt certain assumptions:

1. WIG Vehicle is considered as a rigid body;
2. The mass of the WIG Vehicle is constant in time;
3. The Earth is considered as a flat ground and at the same time an inertial reference system.

With the adopted assumptions, it is possible to apply two basic theorems of classical Newtonian mechanics:

1. The sum of all external forces acting on the observed object is equal to the change in linear momentum over time
$$\sum F = \frac{dQ_s}{dt} \tag{16}$$
2. The sum of all external moments acting on the observed object is equal to the change in angular momentum over time
$$\sum M = \frac{dK_s}{dt} \tag{17}$$

Taking into account previously adopted reference systems, analysed forces, moments and aerodynamic coefficients, the equations of the model in the state space are:

$$\begin{gathered}
\dot{u} = -\frac{1}{2}\rho V_a^2 \frac{S}{m}(C_D \cos\alpha\cos\beta + C_Q\cos\alpha\sin\beta - C_L\sin\alpha) + \frac{F_{t1}+F_{t2}}{m} - g\sin\theta - qw + rv \\
\dot{v} = -\frac{1}{2}\rho V_a^2 \frac{S}{m}(C_D\sin\beta - C_Q\cos\beta) + g\sin\phi\cos\theta - ru + pw \\
\dot{w} = -\frac{1}{2}\rho V_a^2 \frac{S}{m}(C_D\sin\alpha\cos\beta + C_Q\sin\alpha\sin\beta + C_L\cos\alpha) + q\cos\phi - pv + qu \\
\dot{p} = \frac{C_l\frac{1}{2}\rho V_a^2 S}{J_{xx}} \\
\dot{q} = \frac{C_m\frac{1}{2}\rho V_a^2 S + (J_{zz}-J_{xx})}{J_{yy}} \\
\dot{r} = \frac{C_n\frac{1}{2}\rho V_a^2 S + (J_{xx}-J_{yy})qp}{J_{zz}} \\
\dot{\psi} = \frac{r\cos\phi + q\sin\phi}{\cos\theta} \\
\dot{\phi} = p + (r\cos\phi + q\sin\phi)\tan\theta \\
\dot{\theta} = q\cos\phi - r\sin\phi \\
\dot{x_c} = u\cos\theta\cos\psi + v(\cos\psi\sin\theta\sin\phi - \sin\psi\cos\phi) + w(\sin\phi\sin\psi + \sin\theta\cos\psi\cos\phi) \\
\dot{y_c} = u\cos\theta\sin\psi + v(sin\psi\sin\theta\sin\phi + \cos\psi\cos\phi) + w(\sin\theta\sin\psi\cos\phi - \sin\phi\cos\psi) \\
\dot{z_c} = -u\sin\theta + v\sin\phi\cos\theta + w\cos\phi\cos\theta
\end{gathered} \tag{18}$$

where $C_D, C_Q.C_L, C_l, C_m, C_n$ represent aerodynamic coefficients, $\frac{1}{2}\rho V_a^2 S$ air pressure, $x = [u, v, w, \phi, \theta, \psi, p, q, r, x_c, y_c, z_c]^T$ state vector and $u = [\delta_e, \delta_a, \delta_r, \delta_{t1}, \delta_{t2}]$ control vector. Presented final system of equations with initial approximations and calculations of system parameter values, shown in table 3, were integrated into two simulation environments: a MATLAB simulator for traditional control techniques and system stability analysis, and a Python one, for AI based control strategies.

4 Control Strategies Overview

There are numerous articles that present a variety of different approaches and techniques used for the solution of the problem of controlling nonlinear systems. However, each of the proposed solutions provides satisfactory results only if applied to certain problem sets and under certain restrictions. Although the analysis and design of nonlinear systems is successfully applicable only to certain groups of problems, it still cannot be generalized to all systems. When looking into the solutions of Wing-In-Ground vehicle control problem, there are several approaches that can be classified based on the control strategies applied, number of controllers used and system representation that are used as well.

4.1 Algorithmic Control Strategies

Algorithmic control strategies for WIG vehicles involve the use of systematic algorithms and control laws to govern the vehicle's behaviour. These strategies leverage mathematical models and algorithms to achieve stability, control, and performance. The algorithmic control strategies provide systematic approaches to address the complexities of WIG vehicle dynamics, offering stability, precision, and adaptability in various operating conditions. The choice of strategy depends on the specific characteristics and requirements of the WIG vehicle and its mission.

4.1.1 Linear Control Strategies

Linear control strategies for WIG vehicles are based on linearizing the system dynamics around an operating point and designing controllers that operate effectively within this linearized framework. Some of the key linear control strategies used for WIG vehicles are:

- Proportional-Integral-Derivative (PID) Control - PID controllers are widely used in linear control systems. They incorporate proportional, integral, and derivative terms to stabilize and control the WIG vehicle's dynamics.
- LQR (Linear Quadratic Regulator) Control - LQR is an optimal control strategy that minimizes a quadratic cost function. It is suitable for WIG vehicles where a linearized model can be employed, and it provides a feedback control law that optimizes the system's performance.
- State Feedback Control - State feedback control involves directly applying feedback based on the system's state variables. Controllers are designed to stabilize and control the linearized WIG vehicle dynamics.
- Output Feedback Control - In cases where not all state variables are measurable, output feedback control utilizes available measurements to estimate the system's state and design controllers accordingly.
- Linear Quadratic Gaussian (LQG) Control - LQG control combines LQR control with Kalman filtering to handle both state estimation and control. It is effective when dealing with noisy measurements and uncertainties.
- Linear Matrix Inequality (LMI) Control - LMIs are used to formulate and solve optimization problems in control design. LMI-based controllers are applicable to linear systems and can ensure

stability and performance under certain constraints.

- Pole Placement Control - Pole placement involves selecting controller gains to place the system's poles in desired locations. This method is used to achieve specific closed-loop performance characteristics.
- Feedback Linearization - Feedback linearization aims to transform the nonlinear system dynamics into a linear form through feedback. This allows the application of linear control techniques to stabilize and control the system.
- Integral Control - Integral control, often combined with other control strategies, helps eliminate steady-state errors in the WIG vehicle's response to disturbances or setpoint changes.

Linear control strategies are valuable when the WIG vehicle's dynamics can be adequately approximated by a linear model. These approaches provide simplicity, stability, and ease of implementation in certain operating conditions. However, they may have limitations in capturing the full range of nonlinear behaviours exhibited by WIG vehicles.

On the other hand, there are papers approaching this problem with decoupling linearized models and focusing on controlling longitudinal or lateral dynamics, such as explained in (Saeed, Ali, & Shah, 2016), (Ingabire & Sklyarov, 2019) and (Nebylov, Panferov, & Brodsky, 2021) where different control approaches to longitudinal dynamics are analysed or (Sir Elkhatem & Naci Engin, 2022) which is concentrated on robust LQR and LQR-PI control strategies based on adaptive weighting matrix selection for a UAV position and attitude tracking control.

4.1.2 Nonlinear Control Strategies

Nonlinear control strategies for Wing-in-Ground vehicles involve methods that address the inherent complexity and nonlinearities associated with their aerodynamics and dynamics. Here are some key nonlinear control strategies employed for WIG vehicles:

- Adaptive Control - Adaptive control techniques are designed to handle uncertainties and variations in the WIG vehicle's dynamics. These methods adjust control parameters in real-time based on the system's changing conditions.
- Sliding Mode Control - Sliding mode control is a robust control technique that involves creating a sliding surface to guide the system's state toward a desired trajectory. It is particularly effective in handling uncertainties and disturbances.
- Backstepping Control - Backstepping is a recursive control methodology suitable for nonlinear systems. It involves designing controllers for progressively smaller subsystems, effectively breaking down the control problem into manageable parts.
- Fuzzy Logic Control - Fuzzy logic control uses linguistic variables and fuzzy rules to represent and control complex and nonlinear systems. It can handle uncertainties and imprecise information effectively.
- Neural Network Control - Neural networks can be employed for modelling and controlling WIG vehicles. These adaptive systems can learn and adapt to the nonlinearities and uncertainties in the vehicle's dynamics.
- Model Predictive Control (MPC) - MPC is an advanced control strategy that utilizes a dynamic model of the system to predict future behaviour. It then computes control inputs to optimize a specified performance criterion. MPC can handle nonlinearities and constraints effectively.

Funded by
the European Union

- H-infinity Control - H-infinity control focuses on minimizing the effect of disturbances on the system. It is a robust control strategy suitable for systems with uncertain and varying dynamics.
- Adaptive Control - Adaptive control algorithms continuously adjust control parameters based on real-time data to handle uncertainties and variations in the WIG vehicle's dynamics.
- Nonlinear Observer-Based Control - Nonlinear observers are used to estimate unmeasured states of the WIG vehicle, which is crucial for feedback control. Observer-based control strategies can enhance the system's stability and performance.
- Decentralized Control - Decentralized control strategies distribute control tasks among different components of the WIG vehicle. This can enhance the overall stability and adaptability of the system.
- Lyapunov-Based Control - Lyapunov-based control methods use Lyapunov functions to analyse the stability of the system and design controllers that drive the system towards a desired equilibrium.

Implementing these nonlinear control strategies allows WIG vehicles to handle the complex, dynamic, and nonlinear nature of their aerodynamics, providing improved stability, performance, and adaptability during operation. Some of the research papers worth mentioning that are dealing with the control challenge in a way of applying linear or nonlinear control strategies to complete nonlinear models described with coupled and time-varying equations such as feedback linearization, LQR and MPC control strategies analysed in (Patria, Rossi, Fernandez, & Dominguez, 2021) and augmented sliding mode control of a fixed-wing UAV investigated in (Pan et al., 2023). The paper (Tran & Nguyen, 2022) presents a mathematical basis for formulating robust backstepping controllers for a strict-feedback form-type model. The RBSC algorithm is designed to achieve robust stability and high precision in controlling the flight path angle of the aircraft. It is based on the backstepping control design approach, which breaks down the control problem into a sequence of subproblems for lower-order systems. The RBSC algorithm uses virtual controls and state feedback laws to ensure stability and performance specifications are met. The paper proposes a RBSC-based control algorithm for the F-16 longitudinal dynamic model using RBSC with optimal gains determined by the Mass Gain Adjustment. Experimental results validate the theoretical development and numerical simulation study. The RBSC-based control method shows benefits in eliminating steady-state error and improving performance compared to existing results. The limitations include a longer rising time compared to a traditional PD controller. Overall, the paper contributes to the understanding and application of backstepping-based control in flight system dynamics.

In literature one can as well find comparative analysis review papers such as (Groß, Kornev, Hahn, Lampe, & Drewelow, 2014) which is comparing stability and safety characteristics of control strategies with and without feedback and useful advice and strategies for control implementation, such as described in (Panferov, Nebylov, & Brodsky, 2019).

4.2 AI based Control Strategies

In this paragraph, an intuitive explanation of Reinforcement Learning (RL), its applicability to the WIG vehicle GNC design, and a rationale of the steps involved in adopting it as a control strategy are provided.

Reinforcement Learning (RL) (Sutton & Barto, 2018) is a machine learning paradigm where an agent learns to make sequential decisions by interacting with an environment. The agent aims to maximize a cumulative reward signal over time through a process of trial and error. RL is particularly well-suited for problems where an agent must navigate and make decisions in an uncertain and dynamic environment, making it a relevant approach for addressing the guidance, navigation, and control (GNC) challenges of Wing-in-Ground (WIG) vehicles.

In the context of WIG vehicles, RL provides a framework for developing control policies that adapt to varying environmental conditions and operational requirements. The state vector, which in our case includes key parameters like position, orientation, and velocities, serves as the basis for decision-making. The control vector, consisting of deflections of control surfaces and thrust forces, represents the actions the agent can take to influence the WIG vehicle's behavior.

Constrained Reinforcement Learning (CRL) (Liu, Halev, & Liu, 2021) becomes crucial in this scenario because real-world applications often necessitate the consideration of constraints that limit exploration or actions in a given environment. The Constrained RL problem can be formulated as follows:

$$\underset{\theta}{max}\ J_R^{\pi_\theta}$$
$$\text{s.t. } a_t \text{ is feasible}$$

Here, J_R represents the expected cumulative reward, and π_θ is the policy to be optimized. The constraints on a_t ensure that the control actions adhere to the physical limitations of the WIG vehicle's control surfaces and engines. An illustration of possible behavioral and control constraints is shown in Figure 7.

To solve this Constrained RL problem, various techniques from the Constrained RL domain can be explored. The Lagrangian Relaxation approach (Liu et al., 2021), commonly used for cumulative constraints, may be employed to penalize constraint violations in the optimization process. Additionally, Interior-point Policy Optimization (IPO) (Liu, Ding, & Liu, 2020) can be considered as it is a first-order constrained optimization method that has shown promise in handling constrained RL problems.

Evaluation metrics mentioned in the Constrained RL domain, such as expected cumulative cost and regret, can be adapted to assess the efficacy of the GNC policy for the WIG vehicle. Moreover, benchmarks like those in the safety gym can be utilized to validate the developed Constrained RL solution in realistic scenarios (Todorov, Erez, & Tassa, 2012; Ray, Achiam, & Amodei, 2019).

Relevant works in Constrained RL, such as the framework presented by Kim et al. (Kim et al., 2023) for training robots in challenging environments, can provide insights into adapting Constrained RL methodologies to the specific challenges posed by the GNC problem of a WIG vehicle. Additionally, theoretical support from works like (Paternain, Chamon, Calvo-Fullana, & Ribeiro, 2019) can guide the implementation of optimization methods in a GNC context.

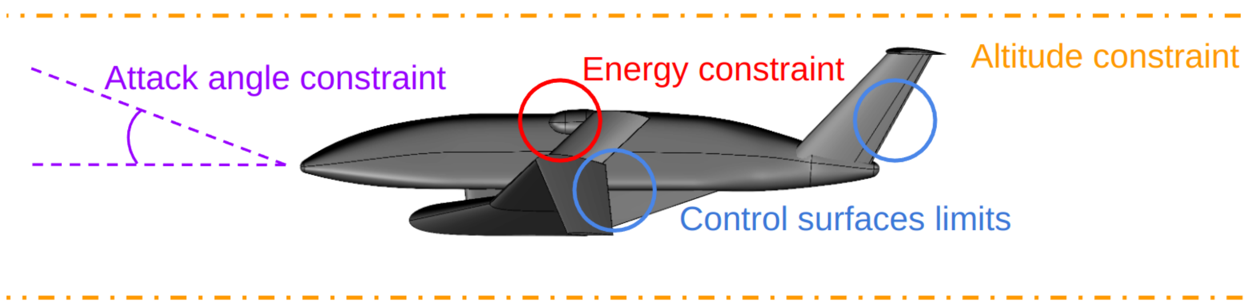

Figure 7: Illustration of potential WIG vehicle constraints for the CRL framework.

The integration of these techniques holds promise for enhancing the autonomy and adaptability of WIG vehicles, contributing to their operational safety and efficiency.

5 Conclusion and Future Work

In this deliverable, the mathematical model for Wing-in-Ground vehicle for extensive simulations of Guidance-Navigation-Control strategies and algorithms is developed and presented. The model offers a framework for analyzing the aerodynamic interactions crucial to the vehicle's operation. By integrating principles from fluid dynamics, aircraft design, and marine engineering, the model provides a solid foundation for understanding the complex dynamics of WIG vehicles as they operate in ground effect. It is important to note that the dynamic model is highly sensitive, meaning small variations in certain parameters can lead to significant changes in observed dynamics. Identifying aerodynamic parameters is challenging, starting with CFD simulations and progressing to physical simulations, such as wind tunnel tests. The resulting estimates may not be universally valid due to variations in the craft's attitude during flight. The developed mathematical model will be used for simulations, which serve as a preliminary stage before physical tests are conducted with WIG vehicle models.

While the current model provides a solid foundation, it is essential to recognize that ongoing tasks will further refine and enhance its accuracy and applicability. Task T3.3, focusing on aerodynamic and hydrodynamic testing, is particularly important in this context. Through wind tunnel and water channel tests, we aim not only to verify and validate simulation results but also to gain deeper insights into phenomena unique to WIG behaviour. The outcomes from these tests will be instrumental in fine-tuning the design parameters of the AIRSHIP-1 and the A0-S prototype, thereby directly contributing to the refinement of the developed mathematical model.

Having in mind that the aim of the upcoming task T5.2 is to achieve fully autonomous control of the WIG vehicle, the choice and implementation of a control strategy to the presented mathematical model is crucial. As described in the previous chapters, the choice of a control strategy depends on various factors, including the specific characteristics of the vehicle, the mission requirements, and the operating conditions. Each control strategy has its advantages and limitations. Ultimately, the selection of a control strategy for a WIG vehicle should involve a thorough analysis of the vehicle's dynamics, the mission objectives, and the environmental conditions. Implementation may also involve a combination of control strategies or adaptive approaches to handle varying scenarios during operation. By combining control strategies and incorporating adaptive elements, WIG vehicles can enhance their ability to handle a variety of scenarios and operating conditions, ultimately improving safety, stability, and overall performance.

In conclusion, research work presented in this deliverable has established the foundational framework for implementing control strategies in the context of Wing-in-Ground vehicles. By addressing key challenges such as intrinsic nonlinearities, time variability of aerodynamic parameters, uncertainties in model featuring, and the high sensitivity of the dynamic model, the groundwork has been laid for the development of robust and adaptive control systems.

Funded by
the European Union

References

Aminzadeh, A., & Khayatian, A. (2017). Stability analysis for time-varying wig craft dynamics in the presence of wavy boundary and gust. *Ocean Engineering*, *145*, 148-157. Retrieved from https://www.sciencedirect.com/science/article/pii/S002980181730481X doi: https://doi.org/10.1016/j.oceaneng.2017.08.031

Caughey, D. A. (2011). Introduction to aircraft stability and control course notes for m&ae 5070.. Retrieved from https://api.semanticscholar.org/CorpusID:113354262

Collu, M., Patel, M. H., & Trarieux, F. (2007). A unified mathematical model for high speed hybrid (air and water-borne) vehicles.

Fevralskikh, A., & Makhnev, M. (2023, March). Determination and analysis of roll and yaw rotary derivatives of wig vehicle using numerical simulation. *Aerospace Systems*, *6*(1), 151–161.

Groß, A., Kornev, N., Hahn, T., Lampe, B., & Drewelow, W. (2014, 07). Flight stability and safety of wig craft with and without feedback control. *ASME 2014 12th Biennial Conference on Engineering Systems Design and Analysis, ESDA 2014*, *1*. doi: 10.1115/ESDA2014-20254

Ingabire, A., & Sklyarov, A. (2019, 01). Control of longitudinal flight dynamics of a fixedwing uav using lqr, lqg and nonlinear control. *E3S Web of Conferences*, *104*, 02001. doi: 10.1051/e3sconf/201910402001

Kim, Y., Oh, H., Lee, J., Choi, J., Ji, G., Jung, M., … Hwangbo, J. (2023). Not only rewards but also constraints: Applications on legged robot locomotion. *arXiv preprint arXiv:2308.12517*.

Komissarov, S., & Gordon, Y. (2020). *Soviet and russian ekranoplans: New expanded edition*. Crecy Publishing Limited. Retrieved from https://books.google.es/books?id=1xWkwwEACAAJ

Liu, Y., Ding, J., & Liu, X. (2020). Ipo: Interior-point policy optimization under constraints. In *Proceedings of the aaai conference on artificial intelligence* (Vol. 34, pp. 4940–4947).

Liu, Y., Halev, A., & Liu, X. (2021). Policy learning with constraints in model-free reinforcement learning: A survey. In *The 30th international joint conference on artificial intelligence (ijcai).*

Moormann, D., Varga, A., Looye, G., & Griibel, G. (1998). For automated lft generation applied to the research civil aircraft model.

Nebylov, A., Panferov, A., & Brodsky, S. (2021). Mathematical model and control system of an ekranoplan under the action of large aerodynamic loads. In *2021 ieee 8th international workshop on metrology for aerospace (metroaerospace)* (p. 516-520). doi: 10.1109/MetroAeroSpace51421.2021.9511756

Pan, Y., Li, N., Zou, W., Wang, B., Wang, K., Tang, X., … Qin, L. (2023). An augmented sliding mode control for fixed-wing uavs with external disturbances and model uncertainties. *Drones*, *7*(7). Retrieved from https://www.mdpi.com/2504-446X/7/7/440 doi: 10.3390/drones7070440

Panferov, A., Nebylov, A., & Brodsky, S. (2019, 06). Features of designing control systems for wig-craft. In (p. 136-141). doi: 10.1109/MetroAeroSpace.2019.8869633

Park, Hyunbum. (2017). Study on design and test of composite wig vehicle considering on impact loading. *MATEC Web Conf.*, *139*, 00022. Retrieved from https://doi.org/10.1051/matecconf/201713900022 doi: 10.1051/matecconf/201713900022

Paternain, S., Chamon, L., Calvo-Fullana, M., & Ribeiro, A. (2019). Constrained reinforcement learning has zero duality gap. *Advances in Neural Information Processing Systems*, *32*.

Patria, D., Rossi, C., Fernandez, R. A. S., & Dominguez, S. (2021). Nonlinear control strategies for an autonomous wing-in-ground-effect vehicle. *Sensors*, *21*(12). Retrieved from https://www.mdpi.com/1424-8220/21/12/4193 doi: 10.3390/s21124193

Phillips, W. F., & Hunsaker, D. F. (n.d.). Lifting-line predictions for induced drag and lift in ground effect. In *31st aiaa applied aerodynamics conference.* Retrieved from https://arc.aiaa.org/doi/abs/10.2514/6.2013-2917 doi: 10.2514/6.2013-2917

Ray, A., Achiam, J., & Amodei, D. (2019). Benchmarking safe exploration in deep reinforcement learning. *arXiv preprint arXiv:1910.01708*, *7*(1), 2.

Rigon Silva, W., da Silva, A., & Gründling, H. (2017, 12). Modelling, simulation and control of a fixed-wing unmanned aerial vehicle (uav).. doi: 10.26678/ABCM.COBEM2017.COB17-2703

Funded by the European Union

Saeed, A., Ali, S., & Shah, M. Z. (2016, 01). Linear control techniques application and comparison for a research uav altitude control.. doi: 10.1109/IBCAST.2016.7429866

Sir Elkhatem, A., & Naci Engin, S. (2022). Robust lqr and lqr-pi control strategies based on adaptive weighting matrix selection for a uav position and attitude tracking control. *Alexandria Engineering Journal*, *61*(8), 6275-6292. Retrieved from https://www.sciencedirect.com/science/article/pii/S1110016821007900 doi: https://doi.org/10.1016/j.aej.2021.11.057

Sutton, R. S., & Barto, A. G. (2018). *Reinforcement learning: An introduction*. MIT press.

Todorov, E., Erez, T., & Tassa, Y. (2012). Mujoco: A physics engine for model-based control. In *2012 ieee/rsj international conference on intelligent robots and systems* (pp. 5026–5033).

Tran, T. T., & Nguyen, V. H. (2022). Nonlinear control of aircraft flight dynamics using integrator-backstepping design method. *Journal of Aerospace Engineering*, *35*(2), 04022001. Retrieved from https://ascelibrary.org/doi/abs/10.1061/%28ASCE%29AS.1943-5525.0001393 doi: 10.1061/(ASCE)AS.1943-5525.0001393

Yang, W., Yang, Z., & Collu, M. (2015, March). Longitudinal static stability requirements for wing in ground effect vehicle. *Int. J. Nav. Archit. Ocean Eng.*, *7*(2), 259–269.

Yun, L., Bliault, A., & Doo, J. (2010a). Longitudinal and transverse stability. In *Wig craft and ekranoplan: Ground effect craft technology* (pp. 189–223). Boston, MA: Springer US. Retrieved from https://doi.org/10.1007/978-1-4419-0042-5_6 doi: 10.1007/978-1-4419-0042-5_6

Yun, L., Bliault, A., & Doo, J. (2010b). Wig craft and ekranoplan. *Ground Effect Craft Technology*, *2*.

Funded by the European Union